

The challenges of using radial inlet guide vanes for wide-range control of a centrifugal compressor

Lukáš Hurda^{1*}, Richard Matas¹, and Matěj Ranš²

¹University of West Bohemia in Pilsen, New Technologies – Research Centre, 30100 Univerzitní 8, Plzeň, Czech Republic

²University of West Bohemia in Pilsen, Department of Power System Engineering, 30100 Univerzitní 8, Plzeň, Czech Republic

Abstract. Regions of significant performance degradation were observed in a single-stage centrifugal compressor tested on a dedicated industrial rig. The machine was operated under discharge throttling, variable impeller speed, and radial inlet guide vane control. The study describes the mechanisms behind the degraded operation and proposes strategies to mitigate the underlying phenomena. Dimensional analysis, zero-dimensional flow models, axisymmetric 2D and 3D CFD simulations, and experimental data evaluation were employed in the research. This work expands on the first author's doctoral dissertation, which provides detailed descriptions of the methods, test facility, and the compressor, as well as a broader set of results. The present article builds on this foundation by establishing deeper connections among the outcomes of different approaches through additional post-processing and new partial analyses.

1 Introduction

Development tests on a centrifugal compressor stage test bed revealed unexpected problems with some, but not all, stages that had been operated under radial variable inlet guide vanes control. The compressor performance dropped in the middle of some of the speed lines; it became noisy, and hysteresis arose in the discharge throttling control. Some speedlines were much narrower than expected. See Fig. 1.

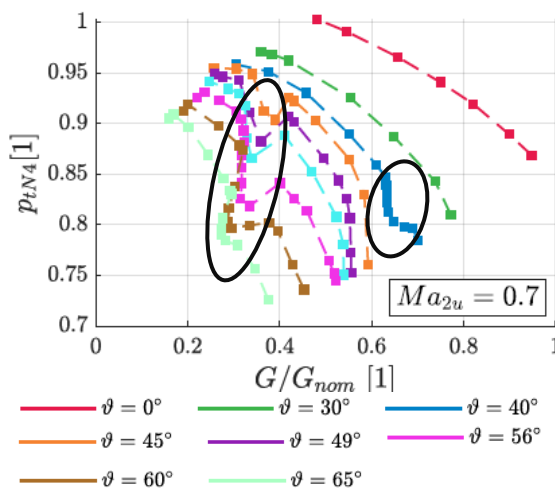


Fig. 1. An example of a set of defective compressor characteristics. Normalised mass flow rate vs. normalised discharge pressure. Speedlines at various IGVs stagger angle. Reference (blade) Mach number of 0.7.

IGVs (inlet guide vanes) are a standard method for operating turbocompressors efficiently over a wide

range of operating regimes. An axial arrangement of IGVs is more common than radial in many applications. However, radial IGVs are clearly beneficial for single-shaft multistage industrial machines, where the winding cross-section of the flow path is typical, and a short shaft is crucial for low costs and easier design. Another typical feature of such machines is a low span-to-chord ratio on the impeller blading of the later stages, as the impeller wheels share both rotational speed and outer diameter, but the compressed fluid becomes denser. It is sometimes unfeasible to use 3D blading with an integrated inducer for such low-span impellers, especially when shrouded impellers are required.

Extensive research was conducted using measurement data analysis, analytical calculation tools, and numerical modelling. In the first author's dissertation [1], such approaches are described in detail.

Dimensional similitude applied to the measurement data confirmed the hypothesis that the defects are not tied to the compressor duty parameters, but rather to the inlet channel swirling flow state.

Further efforts described the mechanism of hub-side flow separation, and, finally, the means to suppress its effects were developed and tested virtually using CFD methods.

One of the proposals is a different impeller geometry, so a new impeller design is demonstrated and subjected to virtual testing.

* Corresponding author: hurda@ntc.zcu.cz

2 Methodology summary

2.1 Experimental setup

The measurement apparatus consisted of total temperature and total and static pressure probes placed at measuring stations, as shown in Fig. 2. Flow rate was measured using a flat plate orifice.

Measurement evaluation algorithms were implemented to correct discrepancies in the rotational speed settings and to scale the gas state at the machine inlet to a standardised one. Methods for describing polytropic compression were examined in [2]. As the programs were developed for more general use within the area of industrial compressors, they implement the real gas equation of state and consider gas humidity, even though the test bed was operated exclusively with atmospheric air.

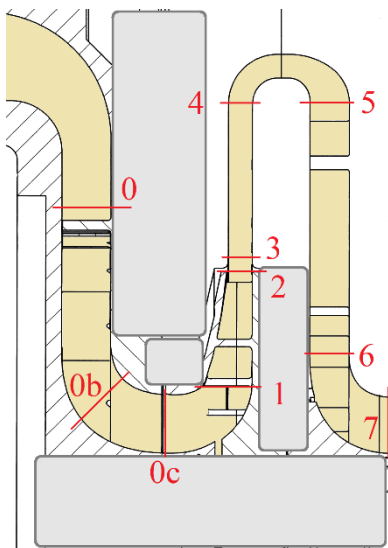


Fig. 2. Single-stage centrifugal compressor cross-section with measuring stations.

2.2 Analytical mean-line flow description

Unlike measurement evaluation, the analytic description of mean-line flow always considers perfect gas behaviour because the explicit linking of state parameters is necessary. It is used to predict the flow parameters along the flow path and evaluate them at stations with a known cross-sectional area. Such apparatus is usually used in turbomachinery design. Here, the focus is on the inlet part of the channel, from the IGVs to the impeller – stations 0 to 1.

Assuming undisturbed flow along the channel mean line, the evolution of the velocity field, total and static state parameters is calculated. To account for the irreversibility of the process, the deviation angle of the flow behind the IGVs and total pressure loss between stations 0b and 1 are modelled as follows:

$$\Delta\alpha_{0b} = 0.1 \cdot \vartheta; \Delta p_{T0b1} = \frac{1}{2} \cdot 1.8 \cdot \rho_{0b} \cdot c_{0b}^2$$

where ρ is gas density, and c is absolute flow velocity. The values of the deviation angle coefficient (0.1 [–]) and total pressure loss coefficient (1.8 [–]) are a qualified estimate.

Notably, the IGVs stagger angle ϑ is not equal to the vane metal exit angle α'_{2IGV} due to the radial arrangement and arbitrary pivot point position. The metal angle at the trailing edge of the IGVs is almost 5° larger at 15° stagger, and this trend intensifies at larger ϑ .

2.3 Computational fluid dynamics

The CFD setup was traditional and simplistic, given the large number of operating points. Steady compressible RANS simulations of periodic domain segments used a moving reference frame for the impeller subdomain. The SST $k-\omega$ two-equation turbulence model was employed. Meshes with fewer than 5 million cells had a good enough resolution to utilise low Re wall treatment.

The total pressure inlet and static pressure outlet with the target mass flow rate algorithm enabled proved robust enough for significantly off-design conditions.

A no-pitch-scale technique enabled the transmission of undistorted flow fields at the non-conformal subdomain interface between the IGVs and the rest of the model. This interface connects static subdomains only; it is intentionally separated from the switch of reference frames. Due to errors emerging at this interface, the IGVs subdomain in the final models involves more than one blade passage to ensure the total pitch angle range of the interface surface is larger than its opposing side.

All the other interfaces were conformal for maximum accuracy. This was also possible thanks to having a bladeless diffuser in the simulated stage.

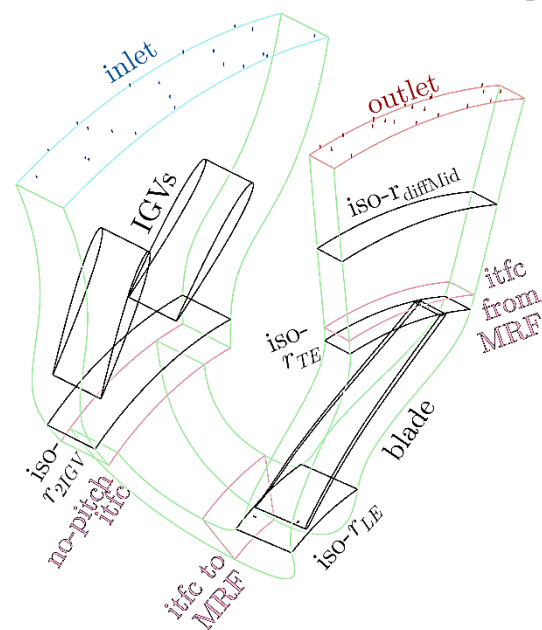


Fig. 3. Outline of the complete CFD model of the compressor stage.

Such complete models of the compressor stage are the pinnacle of CFD analyses involved in this research. Incompressible simplified bladeless channel flow is discussed in [3]. An analysis of the behaviour of only the IGVs was conducted as a prerequisite to modelling the stage without them and enforcing the inlet flow swirl

via the inlet boundary condition. This is also discussed in the results chapter.

2.4 Impeller design

Not just the new impeller was designed, but also a substitute for the original one, as the geometry data were not fully available.

The design was created in multall-open, a software tool published by Prof. John Denton [4]. Only the design tools meangen (mean-line flow designer) and stagen (3D stage geometry generator), were used; the CFD solvers included in the software were not used.

The design point was known approximately. The hub surface was extracted from a blueprint, and a shroud surface conforming to the original was created through manual iterations of the evolution of the meridional speed. The metal angles were matched closely by setting incidence and deviation angles within reasonable ranges. The resulting substitute for the original impeller has a slightly larger wrapping angle (i.e., the transition from the inlet to the exit metal angle is smoother).

With minor adjustments, the channel shape was adopted for the newly designed impeller, and efforts were made to match the compressor stage duty with the original stage, despite the blading being significantly reshaped. See the resulting geometries in Fig. 4.

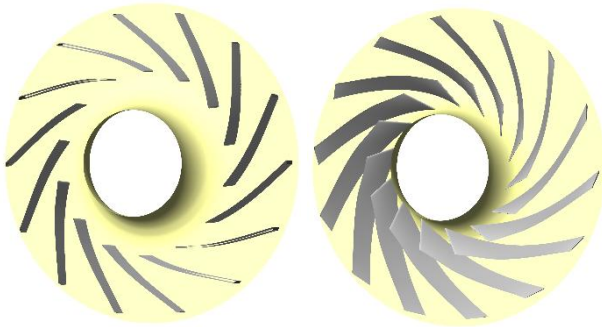


Fig. 4. Original impeller substitute (left), new impeller (right).

3 Results

Here, the most important findings of the first author's dissertation are discussed in brief, and a new correlation between analytical mean-line flow model outcomes and CFD results is presented.

3.1 Impeller blading study

3.1.1 Main hypothesis construction

The progression from simple to more complex flow descriptions revealed that the observed speedline defects are due to hub side flow separation (illustrated in Fig. 5). This is not tied to the compressor duty parameters, but rather to the IGVs and inlet channel flow parameters. Despite this, some stages seemed immune to this flow feature, which can emerge at most of the reasonable operating points at various stages, if the swirl angle is high enough.

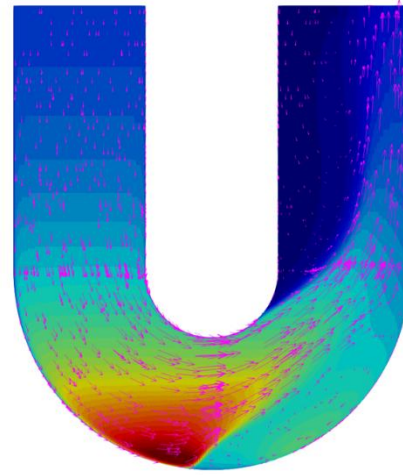


Fig. 5. Illustration of hub side separation in simplified bladeless channel – showing meridional velocity vectors and normalised tangential velocity contours.

The resilient stages were mainly those with a wider channel, i.e., a larger flow capacity. However, the wide channel itself proved to be prone to hub-side separation as well.

The key difference between the narrower stages was the impeller blading geometry – 3D blades with an integrated inducer in contrast to the prismatic blades with a leading edge at a constant radial coordinate.

Therefore, the design of the new impeller focused on creating an integrated inducer with a leading edge shifted upstream into the inlet channel bend, with the hope of suppressing the hub-side vortex.

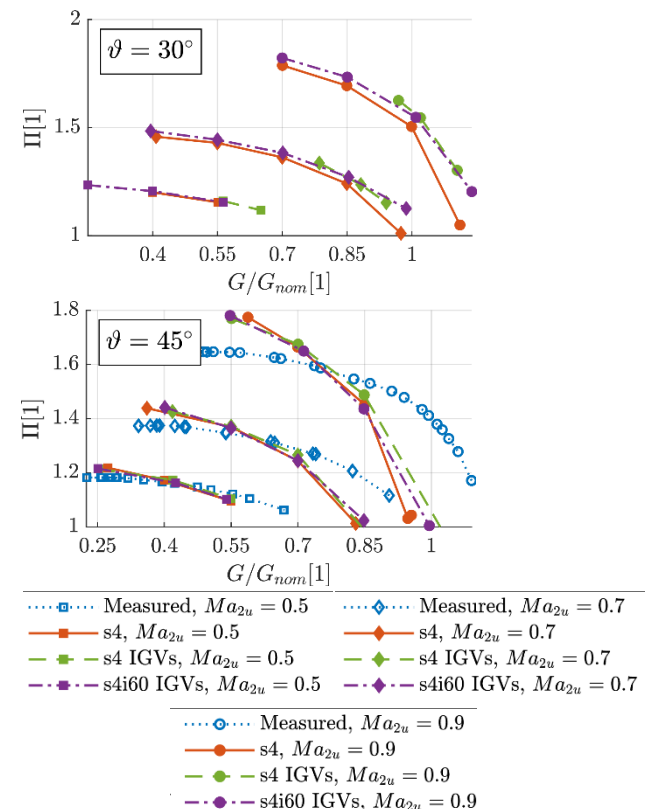


Fig. 6. Measured and computed compressor characteristics.

3.1.2 Experimental and numerical modelling results

Unfortunately, the most carefully measured stage, whose characteristics are shown in Fig. 1, was equipped with a reduced set of sensors, therefore a similar stage was selected. However, the approach of the test bed team at this stage was not to measure the defects, but rather to skip them.

The failure of a CFD model at a particular operating point is considered an indication of harsh flow conditions, which would ultimately result in a real-world compressor duty defect.

Four sets of speedlines are presented – the ‘measured’, the CFD model with original impeller and BC-induced swirl (‘s4’), the original impeller with IGVs included in the model geometry (‘s4 IGVs’), and finally a new impeller with IGVs included (‘s4i60 IGVs’).

It was found that the presence of the wakes of the IGVs play a significant role in the operating point stability. This is pronounced in the $\vartheta = 30^\circ$ graph in Fig. 6, where ‘s4 IGVs’ speedlines are very short.

Fig. 7 illustrates the varying wake propagation abilities at different IGV stagger angles in the channel bend apex axis-normal section, which explains the pronounced effect observed at a 30° stagger.

The new impeller proves to be effective in suppressing the inlet channel vortex.

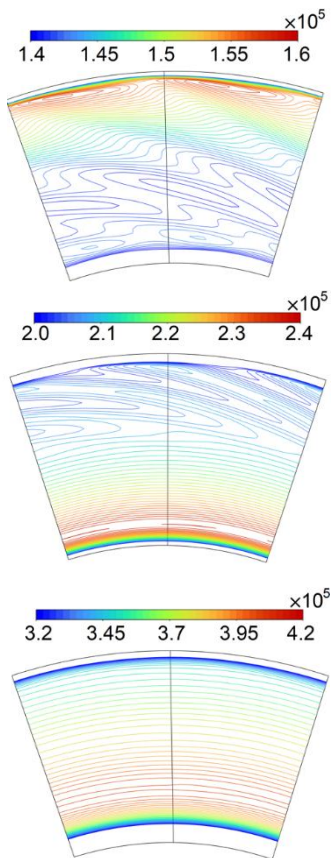


Fig. 7. Local Reynolds number based on channel width at 30° , 45° and 60° IGVs stagger angle (top to bottom) showing the flow disturbance caused by IGVs

3.2 Flow angle and Mach number correlations

An interesting feature of compressor swirling inlet channel flow was discovered through a numerical experiment using a mean-line flow model. Based on the fluid properties, flow rate, channel dimensions, and last but not least the impeller leading edge geometry, a non-monotonous trend of relative Mach number at the compressor inlet can occur across the span of a given speed line. In Fig. 8, a speedline can be imagined as a vertical slice through a constant IGV stagger angle. The indices of the Mach numbers include u and w , representing the impeller circumferential speed and flow velocity relative to the impeller respectively.

The minima of the convex curves of the evolutions of the relative Mach number can be reached at very different incidence angles. These two parameters are seen as key to determining the feasibility of the operating point.

The purely analytical data presented in Fig. 8, published in [1], are sliced at constant IGV stagger angles and correlated with the same values gained from the ‘s4 IGVs’ CFD model simulations – see Fig. 9. The CFD data are taken as mass-averaged averages over the ‘iso- r_{LE} ’ surface seen in Fig. 3.

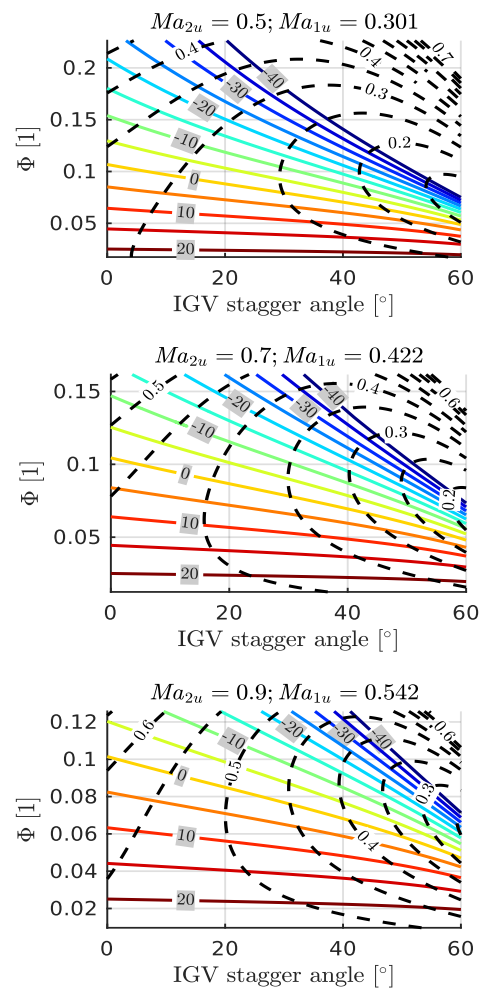


Fig. 8. Leading edge incidence angle $[\circ]$ (coloured isocurves) and relative flow Mach number $[1]$ (dashed black isocurves) for the s4 impeller mean-line flow calculation.

Naturally, all the CFD speedlines are much shorter than those which can be calculated from the compressor's total range of operation. This gives the needed context for the mean-line calculated data.

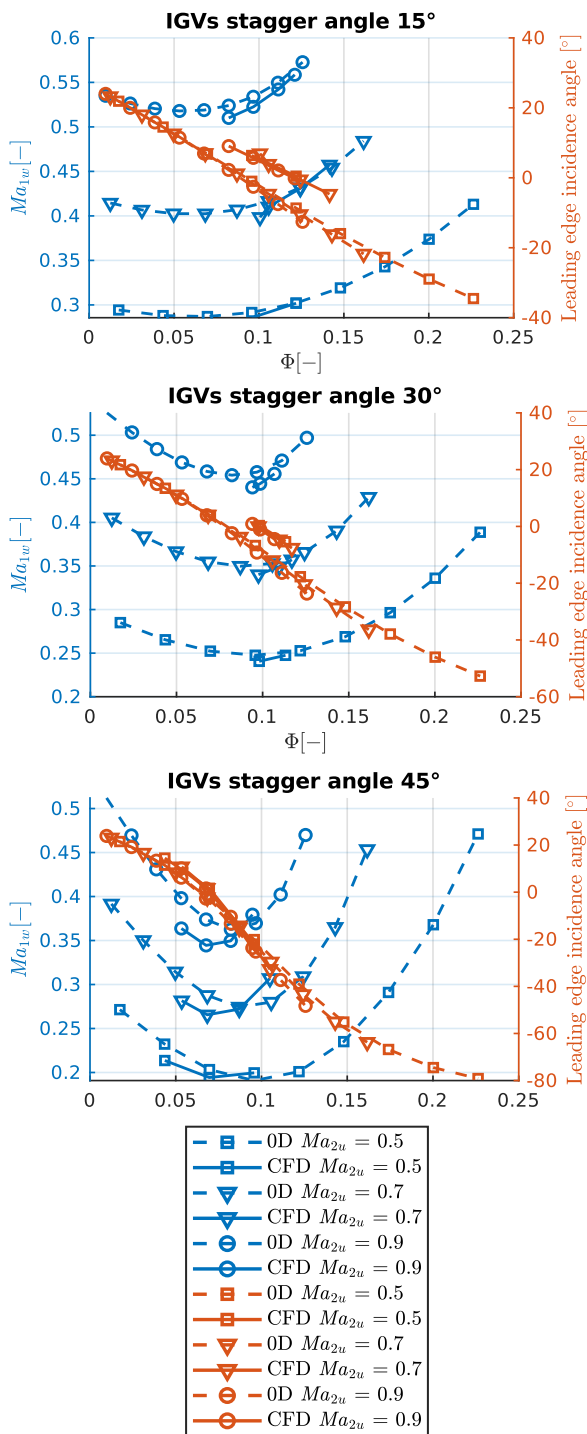


Fig. 9. Correlation of mean-line flow (0D) and CFD data of relative flow Mach number and impeller blade incidence angle plotted against the local flow coefficient.

Overall, the agreement of the Mach number values is satisfactory. The incidence angle predicted by the analytic calculation surprisingly has a larger offset to CFD in lower stagger cases than in larger stagger cases. A global flow coefficient definition is used throughout this evaluation: $\Phi = G/(\rho_0 A_0 u_2)$, where G is mass flow rate, A_0 is the flow area of station '0', and u is used for

impeller circumferential velocity at a respective station. A local flow coefficient evaluated locally at the rotor LE from meridional velocity ($\Phi = c_{m1}/u_1$) has proven to be less practical.

We treat the speedlines always from right-to-left (as measured under discharge throttling from choke to surge):

- At 15° IGVs stagger, Mach is high, but ever-decreasing along speedlines. The incidence reaches a high level for the CFD data, but the operation remains stable due to the absence of problems with the hub-side vortex.
- At 30° IGVs stagger, the characteristics are narrow due to the emerging hub-side vortex, supported by the irregularity of the propagated IGV wakes. Additionally, the Mach number reaches a minimum and may begin to rise at the end of the CFD speedlines, where a further decrease in flow rate causes the simulation to fail.
- At 45°, the situation is similar to that at 30°; however, the Mach values are generally lower, and we can expect a reduced influence of IGV wakes, even though hub-side separation remains present.

There is no conclusive evidence that the compressor duty does not approach a surge limit, along with a decreasing flow rate. Unfortunately, the 's4' stage did not exhibit defects at higher flow rates, well away from surge, as observed for a different stage shown in Fig. 1. This was already commented on in subsection 3.1.2. However, the top part of Fig. 6 partly proves that similar CFD models can reach much lower flow rates to the 's4 IGVs' discussed in this subsection.

4 Conclusions

The phenomenon behind compressor characteristic defects was discovered, described, and an attempt was made to predict their occurrence.

The dimensional similitude proved to be a powerful tool for generalisations, but since three effects need to be linked, the final solution to predictions is not yet clear.

The occurrence of hub side flow separation in front of the impeller and the impeller's ability to handle the blocked inlet flow needed to be correlated with the intensity of the IGV wake effects in the vicinity of the channel bend apex and the impeller inlet to explain the speedline defects.

A newly designed impeller with an integrated inducer, although possibly impractical for manufacturing, managed to suppress the hub-side vortex's adverse effect on the speedlines at a 30° stagger in our set of simulations. It is risky to use the prismatic blading in conjunction with IGVs in a radial arrangement.

Many findings incorporated in this methodology will be taken to conduct further research in this topic.

Acknowledgments

The authors wish to thank Howden ČKD Compressors for kindly allowing the publication of research based on their documentation and measurement data.

The results were developed within the specific research grant UWB SGS-2025-013.

References

1. Lukáš Hurda, Analysis of flow induced instabilities in a centrifugal compressor stage with radial inlet guide vanes, PhD thesis, University of West Bohemia in Pilsen, Faculty of Mechanical Engineering, (2023)
2. L. Hurda, R. Matas, Radial compressor test data processing with real gas equation of state, in AIP Conference Proceedings 2189, Melville, NY, USA: American Institute of Physics Inc., (2019), ISBN 978-0-7354-1936-0, ISSN 0094-243X. doi:10.1063/1.5138621.
3. L. Hurda, R. Matas, Preliminary computational study of centrifugal compressor inlet flow instabilities with radial inlet guide vanes, in proceedings of Power Systems Engineering Conference, Pilsen, CZE (2020)
4. J. Denton, Multall: An Open Source, CFD Based, Turbomachinery Design System, in proceedings of Turbo Expo: Power for Land, Sea, and Air, June (2017), doi: 10.1115/GT2017-63993